Anal Bioanal Chem (2008) 391:2703–2709
DOI 10.1007/s00216-008-1994-z

ORIGINAL PAPER

Incubation type Si-based planar ion channel biosensor

Tsuneo Urisu · Toshifumi Asano · Zhenlong Zhang · Hidetaka Uno · Ryugo Tero · Han Junkyu · Isoda Hiroko · Yusuke Arima · Hiroo Iwata · Koji Shibasaki · Makoto Tominaga

Received: 15 December 2007 / Revised: 13 February 2008 / Accepted: 18 February 2008 / Published online: 5 April 2008

Abstract A new planar-type ion channel biosensor with the function of cell culture has been fabricated using silicon on an insulator substrate as the sensor chip material. Coating of the sensor chip with fibronectin was essentially important for cell incubation on the chip. Although the seal resistance was quite low (~7 MΩ) compared with the pipette patch-clamp giga-ohm seal, the whole-cell channel current of the transient receptor potential vanilloid type 1 (TRPV1) channel expressing HEK293 cells was successfully observed, with a good signal-to-noise ratio, using capsaicin as a ligand molecule.

Keywords Ion channel biosensor · SOI · Extracellular matrix · Fibronectin · Nystatin

T. Urisu (✉) · R. Tero
Institute for Molecular Science, Myodaiji,
Okazaki 444–8585, Japan
e-mail: urisu@ims.ac.jp

T. Urisu · T. Asano · Z. Zhang · H. Uno · R. Tero · K. Shibasaki · M. Tominaga
The Graduate University for Advanced Studies, Myodaiji,
Okazaki 444–8585, Japan

H. Junkyu · I. Hiroko
Alliance for Research on North Africa,
Graduate School of Life and Environmental Sciences,
University of Tsukuba,
1–1–1 Tennodai,
Tsukuba, Ibaraki 305–8572, Japan

Y. Arima · H. Iwata
Institute for Frontier Medical Sciences, Kyoto-University,
53 Kawahara-cho, Shogoin,
Sakyo-ku, Kyoto 606–8507, Japan

K. Shibasaki · M. Tominaga
Okazaki Institute for Integrative Bioscience,
5–1 Higashiyama, Myodaiji,
Okazaki 444–8787, Japan

Introduction

The pipette patch-clamp is an extremely powerful and already established technique for investigation of many electro-physiological subjects such as cell biological functions, neural cell signal transduction characteristics, and effects of chemical compounds on ion channels. However, it is almost impossible to apply this technique to multi-point measurements such as high-throughput screening. To overcome this weak point of the pipette patch-clamp technique, planar type patch-clamp techniques have been proposed [1–11].

The planar patch-clamp technique not only has good prospects for high-throughput screening in drug discovery, but also has a potential attractiveness for investigation of cell functions by measuring several cell-biological parameters at the same time. Many groups have attempted to fabricate planar patch-clamp substrates from various materials [1–7], and some commercial planar patch-clamp devices are already available [8–11]. However, the very short life of the cells directly attached to the substrate is a serious problem in this method. From the viewpoint of applying the planar type patch-clamp biosensor to cell function analysis, it is of great importance to increase the lifetime of the attached cell.

The electrical resistance of the narrow extracellular space in brain tissue affects the propagation of neuronal excitation in dendrites and axons and also the electrical interaction of neurons and glia cells [12], yet little is known about it. Giaever et al. determined the impedance between electrodes with cultured cells on them using the electric cell-substrate impedance-sensing (ECIS) method [13, 14]. Wegener et al. evaluated the resistance by impedance measurement of confluent cell layers grown on gold-film electrodes [15]. In the reports of these experiments, however, the measured

resistances contained the contributions from many cells attached and spread on the electrodes Fromherz et al. determined the sheet resistance of the cleft between the single cell membrane and the substrate surface by measurement of voltage-transfer from cells to silicon chips [16, 17], from the bath to silicon chips [18] using field-effect transistors, and from silicon chips to cell membranes using voltage-sensitive dyes [12, 19]. Although the resistances of the cleft under individual cells adsorbed on the substrates were evaluated in these reports, it is impossible to precisely measure the ion channel current using these methods.

Fibronectin (FN) is an intracellular matrix glycoprotein known to improve cell attachment and spreading [20]. The FN molecule consists of two almost identical subunits, which are composed of three types of module (Type I, Type II, and Type III) arranged like a string of beads and crosslinked close to the C-terminus by disulfide bridges [21]. The most important module is Type III, which contains the arginine–glycine–aspartic acid (RGD) recognition sequence. RGD has been identified as a key motif interacting with cells [21]. The materials coated with FN are promising as substrates for cell-based sensors or tissue engineering [22]. There are many reports attesting to enhanced cell attachment and spreading on the FN-coated substrate surfaces [23–32]. For immobilization of FN on various materials surfaces, different methods have been used. Adsorption is the most commonly used method, because it is convenient and less damaging to the conformation of the adsorbed molecules [32].

In this study, silicon-on-insulator (SOI) substrates in planar type ion channel biosensors [7] were modified with FN. The FN-coated substrates were characterized by AFM and cell spreading assays, which indicated that the substrates are suitable for cell adhesion and spreading by incubation. After the cell covered the pore and spread, the resistance of the cleft between the cell membrane and substrate surface was measured and compared with calculated values. The perforated whole-cell configuration was then formed by the application of nystatin, and the whole-cell current of TRPV1 channel expressing HEK 293 cell spread on the pore activated by capsaicin was recorded.

Materials and methods

Preparation of substrates

The thicknesses of the Si and SiO_2 (box) layers of the SOI substrates were 3±0.5 and 3.9±0.2 μm, respectively. The resistivity of the SOI layer was 50–75 Ωcm. The fabrication of the substrate is described in detail in the previous report [7]. In brief a 0.2 μm thick SiO_2 layer was formed on the SOI substrate surface by thermal oxidation at 900 °C with water-saturated O_2 flow. A large well on the reverse side was made by diamond drilling. Subsequently the pyramid-shaped hole was formed by the 8% (*v*/*v*) TMAH etching at 90 °C for about 40 min, which reaches the buried SiO_2 layer. Finally a micro-pore of diameter 1.2 to 1.5 μm in the silicon membrane was made by focused ion beam (FIB) milling from the reverse side. After each use, the substrates are cleaned again for recycling by dipping into acetone and methanol for 20 min each, then placing in boiling piranha solution (H_2O_2:H_2SO_4 1:4, *v*/*v*) for 20 min, thoroughly rinsed with deionized water, dried with nitrogen, and sterilized by ultraviolet light.

FN-coating on the substrate surface

Fibronectin from human plasma, lyophilized from 0.05 mol L^{-1} Tris-buffered saline, pH 7.5, was obtained from Sigma–Aldrich (St Louis, MO, USA). The FN vial was first equilibrated at room temperature and dissolved in sterile deionized water for at least 30 min at a concentration of 1 mg mL^{-1}. The dissolved FN solution could be stored in working aliquots at −20 °C. The working aliquot was diluted in phosphate-buffered saline (PBS) at 500 μg mL^{-1} concentration before use. For FN adsorption by the substrate surface, a droplet of fibronectin solution was put on the substrate and incubated for 1 h at 37 °C followed by rinsing with sterile deionized water, then dried in air. All the operations were performed on a clean bench.

An SPI 3800 scanning probe microscope (Seiko Instrument) was used to analyze the topography and roughness of the substrates before and after coating with FN. Images were obtained in the dynamic force mode (tapping mode) using an Si cantilever with spring constant of 36 N m^{-1} and resonance frequency of 338 kHz.

Cell spreading

Human embryonic kidney 293 (HEK-293) cells were transfected with transient receptor potential vanilloid type 1 (TRPV1). The cells were cultured in a dish filled with Dulbecco's modified Eagle's medium (DMEM, Sigma–Aldrich) at 37 °C in 5% CO_2. In these experiments, DMEM was always supplemented with 10% (*v*/*v*) fetal bovine serum (FBS, Biological Industries), 1% (*v*/*v*) gluta max (Gibco), 0.5% (*v*/*v*) penicillin–streptomycin (Gibco), and 500 mg mL^{-1} geneticin (G418, Gibco)

For cell spreading, HEK-293 cells from a dish were prepared as follows. The culture medium was removed by aspiration and the cells were washed twice with phosphate-buffered saline (PBS, Wako). The cells were then incubated in trypsin–EDTA (Gibco) for 3–4 min in an incubator at 37 °C and detached from the dish surface by agitating several times. The cells were then transferred to a conical

centrifuge tube and spun down at 1000 rpm for 5 min. Finally the cells were suspended in DMEM supplemented with 10% FBS. HEK 293 cells were placed on the FN-coated substrates and incubated at 37 °C with 5% CO_2.

Actin staining

HEK 293 cells were distributed on the FN-coated substrates and incubated at 37 °C in 5% CO_2 in an incubator for 24 h, 48 h, and 72 h. They were washed with PBS, fixed with 3.7% formaldehyde (HCHO, in PBS) for 5 min, permeabilized in 0.2% Triton X-100 (in PBS) for 5 min at room temperature, and then washed with PBS three times. Cells on the substrate were stained for 30 min in 70 nmol L^{-1} fluorescent phalloidin (in PBS) at room temperature. Cells were then washed three times. Finally a droplet (about 25 μL) of Vectashield hard set mounting medium with DAPI (Vector Laboratory) was added to the cell and the substrate was covered with a cover glass.

Cell spreading on the pore of the substrate

After being coated with FN, the planar patch-clamp substrate was assembled in the chamber shown in Fig. 1. DMEM was then injected into the upper chamber and the lower chamber followed by checking of the conductivity of the pore with an amplifier. Care was taken to remove the bubbles in the solution. The cell suspension in DMEM was then put in the upper chamber. After about 10 min the pore was covered by one of the cells brought by the water flow through the pore from the upper chamber to the lower chamber. The upper chamber was then covered with a cover glass to protect the cell from contamination. All operations were performed on a clean bench. After confirming, with the microscope, that the cell was covering the pore, the system was put into the incubator at 37 °C with 5% CO_2 for incubation. After 2 h, the system was taken out to check the spreading condition of the cell on the pore and the seal resistance was measured.

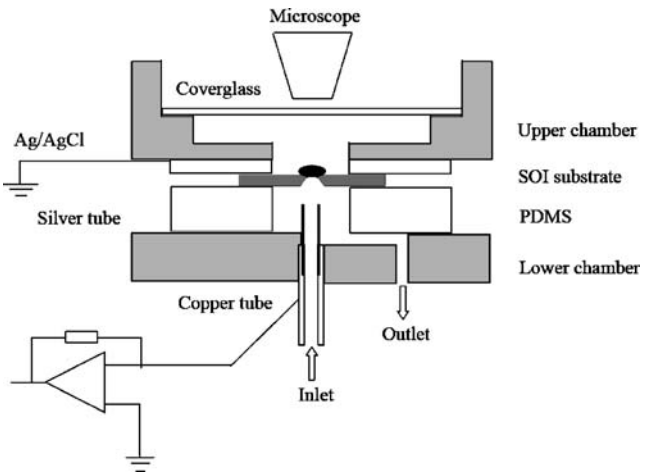

Fig. 1 Schematic structure of the planar type ion channel biosensor fabricated in this work

Preparation of nystatin

Nystatin (Sigma–Aldrich) [33, 34] (10 mg) was dissolved in 1 mL methanol and HCl (1 mol L^{-1}, 45 μL) was added to the solution followed by addition of NaOH (1 mol L^{-1}, 45 μL). The nystatin stocks were diluted to 200–500 μg mL^{-1} with pipette solution before use. Refrigerated nystatin methanol stocks were used within two weeks and the final pipette solution was used within 2 h of preparation.

Electrical measurements

Currents were recorded with the Axopatch 200B (Axon Instruments) and the Digidata 1322A (Axon Instruments). All traces were obtained with a filter frequency of 500 Hz. A fluorescence microscope (Olympus BX51W1) was used for optical measurement.

Results and discussion

Characterization of FN adsorption and cell spreading

Figure 2 shows the atomic force microscope (AFM) images of the substrate surface before and after coating with 500 μg mL^{-1} FN solution. The observed surface roughnesses of the substrates were 0.12 nm and 1.91 nm, respectively.

Figure 3 shows the optical microscope images of cell spreading on the silicon substrates without FN-coating (Fig. 3a and b) and with FN-coating (Fig. 3c and d). These assays were performed at the same cell concentrations of 5×10^5 cells mL^{-1}. It can be seen that the number of cells on the FN-coated substrate are larger than those on the substrate without FN-coating. Moreover the cells adsorbed on FN-coating substrate are distributed uniformly, whereas

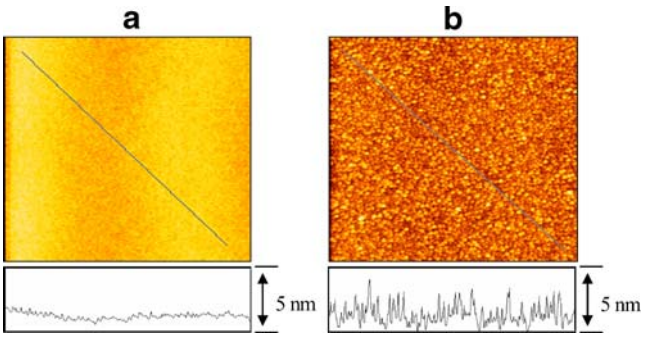

Fig. 2 AFM images (*top*, 5 μm×5 μm) and line scans (*bottom*) of the substrate surface. (**a**) The silicon substrate without FN-coating. (**b**) After being coated with FN, the roughness of the substrate surface increases to 1.91 nm

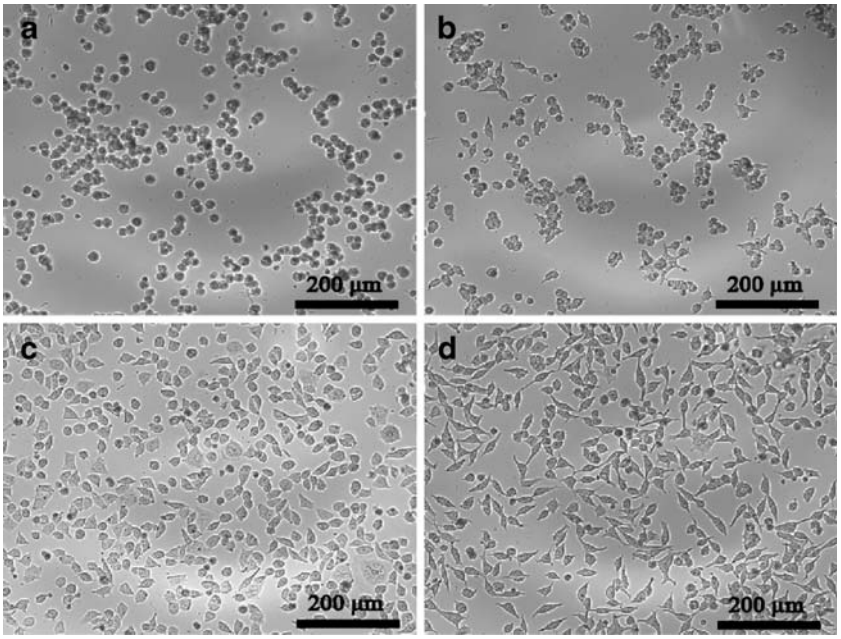

Fig. 3 Optical microscope images of cell adsorption and spread on silicon substrates without FN-coating (**a, b**) and with FN-coating (**c, d**). Incubation times: (**a**) and (**c**) 2 h, (**b**) and (**d**) 5 h

cells on the substrate not coated with FN are prone to aggregate. The cells adsorbed on the FN-coated substrate spread after 2 h incubation (Fig. 3c), whereas only a fraction of the cells on the substrate not coated with FN spread even after incubation for 5 h (Fig. 3b).

Cytoskeleton formation can be analyzed by selective staining of F-actin of the HEK 293 cells. Figure 4 shows the fluorescence microscope images of the cells after incubation for 24, 48, and 72 h. The red color indicates the F-actin stained with fluorescent phalloidin and the blue indicates the cell nuclei stained with DAPI. The F-actin is completely formed after 72 h culture and fully spread cells display cytoskeleton organization.

Cell spread on the pore of the substrate and resistance of the cleft

Figure 5a shows the schematic cross section of a cell spreading on the pore of FN-coated planar patch-clamp substrate. Cell membrane is separated from the substrate by a cleft with a thickness of d_J. The cleft is filled with an electrolyte with a resistivity ρ, which gives a resistance R_J. The equivalent circuit of the cell–substrate junction is illustrated in Fig. 5b, in which R_m and C_m are the resistance and capacitance, respectively, of the cell membrane, C_s is the capacitance of the substrate, R_J is the resistance of electrolyte in the cleft between the cell and the substrate surface, R_a is the access resistance, and R_m is approximated as infinite compared with R_J. The seal resistance can be therefore estimated by use of Eqs 1–3:

$$R_s = R_a + R_J = R_1 + R_2 + R_J \tag{1}$$

$$R_1 = \rho \frac{l_p + d_J}{\pi \cdot r_p^2} \tag{2}$$

$$R_2 = \frac{4\rho L}{2\pi L(\tan\varphi)D + \pi D^2} + \frac{\rho}{2D} \tag{3}$$

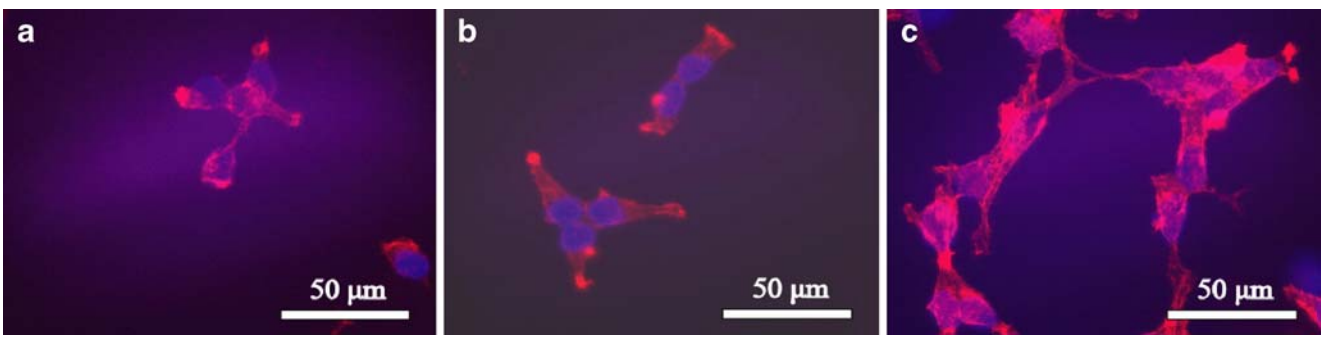

Fig. 4 Fluorescence microscope images of the stained cells on FN-coated substrates after cell culture for (**a**) 24 h, (**b**) 48 h, and (**c**) 72 h. The cytoskeleton organization and actin fibers are formed on FN-coated substrates

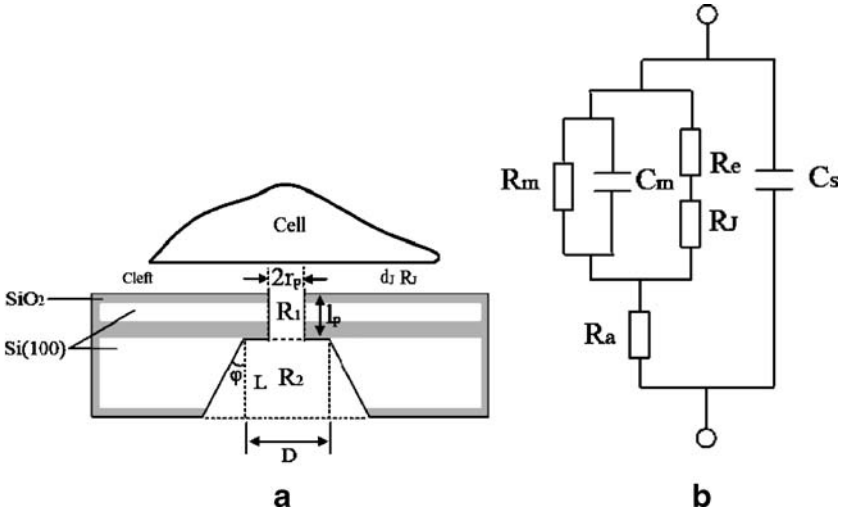

Fig. 5 (**a**) Schematic cross section of a cell spreading on the pore of an FN-coated planar ion-channel biosensor substrate. The cell membrane is separated from the substrate by a cleft of thickness d_J. The cleft is filled with an electrolyte of resistivity ρ. The resistance of the electrolyte in the cleft is R_J. R_1 and R_2 are the resistances of the micropore region and the well region, respectively. L is the depth of the well. r_p and l_p are the radius and the length of the micropore, D is the side length of the bottom square of the well formed by TMAH etching, and φ is the half of the conical angle. (**b**) Equivalent circuit of FN-coated substrate and cell contact. R_m and C_m are the resistance and capacitance, respectively, of the cell membrane. C_s is the capacitance of the substrate. R_a is the access resistance which is given by $R_1 + R_2$. R_e is the additional resistance originating from the narrow gap between neighboring cells, which appears only when the confluent cell layer is formed

where the total seal resistance is R_s, the resistance resulting from electrolyte in the pore is R_1, the resistance resulting from the electrolyte in the well is R_2 [35], the pore length is l_p, and the pore radius is r_p. The depth of the well L, the side length D of the bottom square with the well formed by TMAH etching, and half of the conical angle, φ, are shown in Fig. 5a. For confluently cultured cells, additional resistance R_e due to the narrow gap between the neighboring cells is added to the total seal resistance R_s. $R_s = R_e + R_J + R_a$. The resistance R_j of the cleft between the cell and the FN-coated substrate can be calculated based on the model shown in Fig. 6, in which the circle with a radius of r_p shows the micropore on the substrate and the irregular figure shows a spreading cell on the pore. The resistance of the sector i in Fig. 6 is given by Eq. 4, and the resistance R_J is given by Eq. 5 with $\theta = 2\pi/n$.

$$R_{(i)} = \frac{\rho}{\theta \cdot d} \ln \frac{r_p + l_i}{r_p} \tag{4}$$

$$R_J = \frac{1}{\sum_{i=1}^{n} \frac{1}{R_{(i)}}} \tag{5}$$

where l_i is the length of each sector.

Figure 7a shows the optical microscope image (sample #1 in Table 1) of the cell spreading on the pore, in which the arrow indicates the pore position. For the cells adsorbed on the FN-coated SiO_2 substrate surface, we assume the thickness of the cleft between the cell and substrate as 75 nm [18] and the resistivity of the electrolyte in the cleft ρ as 0.72 Ωm [36]. In the model shown in Fig. 6, since the calculated resistance R_J gives an almost constant value for $n > 80$, $n = 100$ is used for calculations of all samples, where n is the sector number defined in Fig. 6. The calculated and

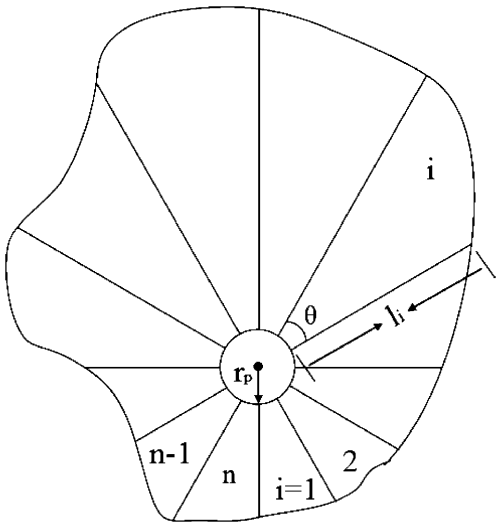

Fig. 6 Model for calculation of the resistance of the cleft of thickness d_J between the cell membrane and the FN-coated substrate. The irregular figure shows a spreading cell on the pore. The sector number is n. $\theta = 2\pi/n$. r_p is the radius of the micropore on the substrate. l_i is the length of the sector i

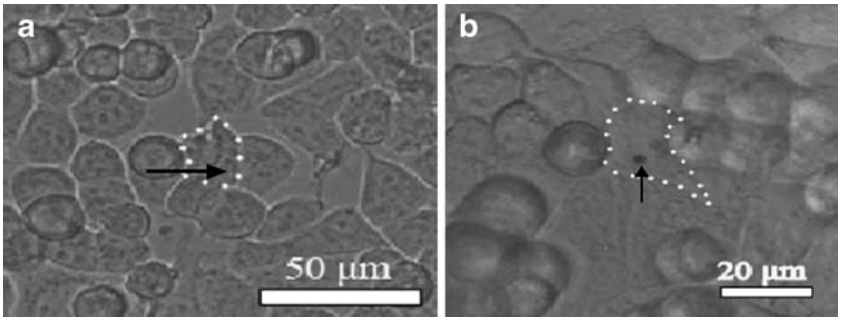

Fig. 7 Optical microscope images of cells spreading on the pores in the substrates. The seal resistance were measured to be (**a**) 6.3 MΩ for sample #1 and (**b**) 8.4 MΩ for the confluent cells. The *arrows* show the positions of the pores. The *white dotted lines* show the cells spreading on the pores. Round cells are sitting on the spreading cells

measured resistance values for three samples are listed in Table 1.

Figure 7b shows the optical microscope image of a layer of confluent cells on the substrate. The black circle indicates the micropore and the white dotted line shows the cell spreading on the pore. In this case, the seal resistance R_s was measured to be 8.40 MΩ and the resistance, $R_J + R_a$, was calculated to be 5.42 MΩ, therefore the effective resistance R_e due to the confluent effect is estimated to be 2.98 MΩ.

Formation of perforated whole-cell arrangement using ionophore and channel current measurements

After spreading of the cell on the pore, gentle suction was applied to draw a cell into the pore. The seal resistance increase during this process was typically 2–4 MΩ. Then DMEM was changed to the bath solution in the upper chamber and to the pipette solution in the lower chamber. An ionophore nystatin was used to form the perforated whole-cell mode by applying it to the lower chamber. Nystatin inserted into the membrane across the pore in the substrate makes the cell membrane electrically permeable without rupturing it. Whole-cell mode formation was certified by monitoring the change of the total capacitance $C_s + C_m$. The total capacitance was typically 100 pF and gradually increased by about 10 pF about 10 min after addition of 200 μmol L^{-1} nystatin solution. Capsaicin (0.5 μmol L^{-1}), the ligand of TRPV1, was then added in the upper chamber and washed out, and the whole-cell current was recorded. Figure 8 shows the whole-cell current of the TRPV1 channel expressing HEK-293 cell activated by repeated capsaicin (0.5 μmol L^{-1}) application and wash out. The first application of capsaicin induces a large current increase, and the current increase induced by the second application is weaker. This behavior agrees well with the report in the literature [37].

Table 1 Calculated and measured resistance of cells spreading on the pores

Sample ($2r_p$, μm)	Calculated (MΩ)				Measured (MΩ)	
	R_1	R_2	R_J	R_s	$R_1 + R_2$	R_s
#1 (1.5)	1.55	0.0028	4.68	6.23	1.3	6.30
#2 (1.2)	2.61	0.0028	4.83	7.44	2.5	7.30
#3 (1.2)	2.61	0.0028	4.67	7.28	2.7	7.40

Discussion

Figure 3 data shows that surface coating by an extracellular matrix protein such as FN is essential for fabrication of the incubation type ion-channel biosensor. The good agreement between calculated and measured values of R_s, as shown in Table 1, indicates that the model of the gap between cell and substrate surface shown in Fig. 5 and the assumed value of the cleft thickness 75 nm are good approximations. In the case of the pipette patch clamp, the high seal resistance, a gigaohm seal, is the important factor when evaluating the performance of the measurement system. In the case of the incubation-type ion channel biosensor, however, a gigaohm seal is difficult to realize due to the existence of the cleft. In the present system, the current noise measured in Fig. 8 was 60 pA. This noise level corresponds to 20–30 channel openings, and indicates that this technique is sufficiently applicable to high-throughput screening for drug discovery. However, since the whole cell current measured in the neural cell signal transducing experiments is usually several tens to

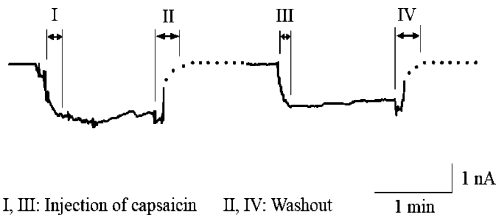

Fig. 8 Observed whole-cell current of TRPV1-transfected HEK-293 cell activated by repeated capsaicin (0.5 μmol L^{-1}) applications. The confluently cultured substrate shown in Fig. 7b is used. Desensitization in the extracellular solution containing Ca^{2+} is observed. Holding voltage is −30 mV. Data are not shown for the dotted line region, where the signal is significantly disturbed by the noise induced by washout operations

hundreds of pA [38], several times lower noise level is desirable when we apply this technique to analysis of neural cell function. Furthermore, the position of the pore almost always deviates from the center of the cell. This may be improved by incubating the cell on the suitably-patterned extracellular matrix protein.

Conclusion

By using a substrate coated with the extracellular matrix protein, FN, planar type ion channel biosensor operation using the cell cultured on the substrate has been successfully demonstrated, although improvements are expected in the current noise characteristics and cell positioning. The good agreement between calculated and measured values of R_s indicates that the model of the gap between cell and substrate surface and the assumed value of the cleft thickness, 75 nm, are good approximations.

Acknowledgements This work was partly supported by NINS Cooperative Project Bio-molecular Sensor, and Grants-in-Aid for Scientific Research, Basic research (A) and Priority Area "Life Surveyor" promoted by the Ministry of Education, Culture, Sports, Science and Technology, Japan.

References

1. Fertig N, Blick RH, Behrends JC (2002) Biophys J 82:3056–3062
2. Sordel T, Raveaud SG, Sauter F, Catherine PC, Marcel F, Waard MD, Arnoult C, Vivaudou M, Chatelain F, D'hahan NP (2006) J Biotechnol 125:142–154
3. Matthews B, Judy JW (2006) J Microelectromechan Syst 15:214–222
4. Pantoja R, Nagarah JM, Starace DM, Melosh NA, Blunck R, Bezanilla F, Heath JR (2004) Biosens Bioelectron 20:509–517
5. Sett A, Burkhardt C, Weber U, Van SP, Knott T (2003) Recept Channels 9:59–66
6. Li XH, Klemic KG, Reed MA, Fred J, Sigworth FJ (2006) Nano Lett 4:815–819
7. Zhang ZL, Asano T, Uno H, Tero R, Suzui M, Nakao S, Kaito T, Shibasaki K, Tominaga M, Utsumi Y, Gao YL, Urisu T (2007) Thin Solid Film 516/9:2831–2833
8. Bruggenmann A, Stoelzle S, George M, Behrends JC, Fertig N (2006) Small 2:840–846
9. Dubin AE, Nasser N, Rohrbacher J, Hermans AN, Marrannes R, Grantham C, Van RK, Cik M, Chaplan SR, Gallacher D, Xu J, Guia A, Byrne NG, Mathes C (2005) J Biomol Screen 10:168–181
10. Willumsen NJ (2006) Am Biotechnol Lab 24:20–21
11. Bridgland-Taylor MH, Hargreaves AC, Easter A, Orme A, Henthorn DC, Ding M, Davis AM, Small BG, Heapy CG, Abi-Gerges N, Persson F, Jacobson I, Sullivan M, Albertson N, Hammond TG, Sullivan E, Valentin JP, Pollard CE (2006) J Pharmacol Toxicol Methods 54:189–199
12. Gleixner R, Fromherz P (2006) Biophys J 90:2600–2611
13. Giaever I, Keese CR (1984) Proc Natl Acad Sci USA 81:3761–3764
14. Lo CM, Keese CR, Giaever I (1995) Biophys J 69:2800–2807
15. Wegener J, Hakvoort A, Galla HJ (2000) Brain Res 853:115–124
16. Weis R, Muller B, Fromherz P (1996) Phys Rev Lett 76:327–330
17. Weis R, Fromherz P (1997) Phys Rev E 55:877–889
18. Kiessling V, Muller B, Fromherz P (2000) Langmuir 16:3517–3521
19. Braun D, Fromherz P (2004) Biophys J 87:1351–1358
20. Potts JR, Campbell ID (1996) Matrix Biol 15:313–320
21. Zhang Y, Chai C, Jiang XS, Teoh SH, Leong KW (2007) Mater Sci Eng C 27:213–219
22. Ruoslahti E, Pierschbacher MD (1987) Science 238:491–497
23. Wittmer CR, Phelps JA, Saltzman WM, Van Tassel PR (2007) Biomaterials 28:851–860
24. Koenig AL, Gambillara V, Grainger DW (2003) J Biomed Mater Res 64A:20–37
25. Miller T, Boettiger D (2003) Langmuir 19:1723–1729
26. Pompe T, Kobe F, Salchert K, Jorgensen B, Oswald J, Werner C (2003) J Biomed Mater Res 67A:647–657
27. Toworfe GK, Composto RJ, Adams CS, Shapiro IM, Ducheyne P (2004) J Biomed Mater Res 71A:449–461
28. Kowalczynska HM, Nowak-Wyrzykowska M, Kolos R, Dobkowski J, Kaminski J (2005) J Biomed Mater Res 72A:228–236
29. Ku Y, Chung CP, Jang JH (2005) Biomaterials 26:5153–5157
30. Lan MA, Gersbach CA, Michael KE, Keselowsky BG, Garcia AJ (2005) Biomaterials 26:4523–4531
31. Calonder C, Matthew HWT, Van Tassel PR (2005) J Biomed Mater Res 75A:316–323
32. Lee MH, Ducheyne P, Lynch L, Boettiger D, Composto RJ (2006) Biomaterials 27:1907–1916
33. Horn R, Marty A (1988) J Gen Physiol 92:145–159
34. Strauss U, Herbrik M, Mix E, Schubert R, Rolfs T (2001) Pflügers Arch-Eur J Physiol 442:634–638
35. Mayer M, Kriebel JK, Tosteson MT, Whitesides GM (2003) Biophys J 85:2684–2695
36. Fuhr G, Müller T, Schnelle Th, Hagedorn R, Voigt A, Fiedler S, Arnold WM, Zimmermann U, Wagner B, Heuberger A (2005) Naturwissenschaften 81:528–535
37. Caterina MJ, Schumacher MA, Tominaga M, Rosen TA, Levine JD, Julius D (1997) Nature 389:816–824
38. Ren M, Yoshimura Y, Takeda N, Horibe S, Komatsu Y (2007) Science 316:758–761